

# Interlaminar Fracture Characteristics of Bonding Concepts for Thermoplastic Primary Structures

John C. Fish,\* Marcia L. Vitlip,† and Stephen P. Chen‡  
McDonnell Douglas Helicopter Company, Mesa, Arizona 85205

and  
Kwang S. Shin§  
Arizona State University, Tempe, Arizona 85287

The fracture characteristics of candidate bonding concepts for thermoplastic structures (APC-2) were evaluated. The concepts covered a wide range of processing requirements (time and temperature). Structural performance was evaluated in mode I and mode II static fracture tests using double cantilever beam and end notched flexure specimens, respectively. The bonding materials included poly-ether-ether-ketone (PEEK) film, poly-ether-imide (PEI) film, and a film adhesive (FM-300). Coconsolidating the APC-2 with PEI prior to secondary bonding with PEI and film adhesive was also considered. Strain energy release rates for crack initiation were calculated for both fracture modes. The PEEK film bond increased the  $G_{Ic}$  and  $G_{IIc}$  initiation values by 100 and 480%, respectively, over the baseline APC-2 laminates. Of the lower temperature bonding concepts, the PEI bond with surface treatment (coconsolidation of PEI with APC-2) was found to provide the best mode I performance (4.1 in.-lb/in.<sup>2</sup>), whereas the film adhesive bond with surface treatment provided the best mode II performance (8.0 in.-lb/in.<sup>2</sup>). Although significant fracture toughness can be retained relative to the composite material (APC-2), increased scatter, particularly in mode I fracture, is inherent in bonded structures.

## Nomenclature

$a$	= effective crack length
$b$	= specimen width
$C$	= compliance
$C_o$	= coefficient for compliance curve fit
$G_{Ic}$	= mode I strain energy release rate
$G_{IIc}$	= mode II strain energy release rate
$h$	= specimen thickness
$L$	= half the distance between outer loading points for end notched flexure specimen
$m_1$	= slope of line for double cantilever beam compliance calibration method
$m_2$	= slope of line for double cantilever beam modified compliance calibration method
$m_3$	= slope of line for end notched flexure compliance calibration method
$P$	= applied load
$\Delta$	= crack length axis intercept
$\delta$	= displacement between load points

## Introduction

McDONNELL Douglas Helicopter Co. (MDHC) is developing thermoplastic primary structures for the next generation of helicopters. A thermoplastic stabilator design currently under development at MDHC is shown in Fig. 1. Low-cost fabrication methods are utilized throughout the de-

sign, and the number of major parts is reduced by 50%, relative to the metal baseline.

One area of great potential for cost reduction is in the joining of structural components, which can be bonded in one operation using low-cost tooling. Secondary bonding concepts at lower temperatures, which minimize tooling requirements, may also be desirable. In addition, different bonding techniques can be applied throughout the structure in an effort to balance cost with performance.

The fracture performance of bonded joints is related to the materials used, design of the structure, and loads on the structure. The fracture of a skin-stiffener joint is illustrated in Fig. 2. The loads and geometry of the structure create specific contributions of mode I and mode II fracture parameters for the joint. These are shown as mode I and mode II strain energy release rates  $G_I$  and  $G_{II}$ , respectively. The magnitudes of the strain energy release rates define the structural performance requirements for the joint. Thus, knowledge of the fracture characteristics associated with selected bonding methods is essential to confidently and efficiently design thermoplastic primary structures.

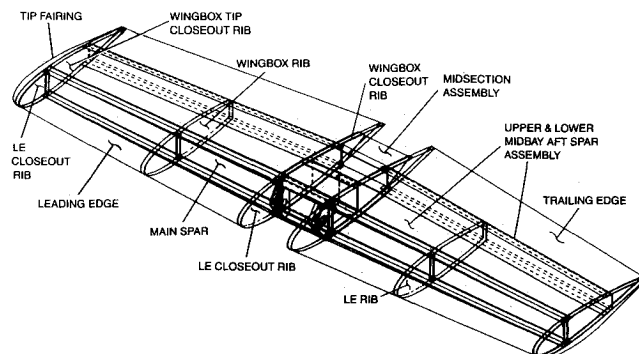


Fig. 1 Thermoplastic horizontal stabilator.

Received May 10, 1991; revision received Sept. 20, 1991; accepted for publication Sept. 22, 1991. Copyright © 1991 by the American Institute of Aeronautics and Astronautics, Inc. All rights reserved.

\*Member, Technical Staff; currently, Senior Design Specialist, Lockheed Advanced Development Co., Department 25-43, Building 311, Plant B-6, P.O. Box 250, Sunland, CA 91041. Senior Member AIAA.

†Member, Technical Staff, Advanced Design Department, Building 530, MS B327, 5000 E. McDowell Road.

‡Member, Technical Staff, Materials and Process Development Department, Building 531, MS C235, 5000 E. McDowell Road.

§Associate Professor, Department of Chemical, Biological and Materials Engineering.

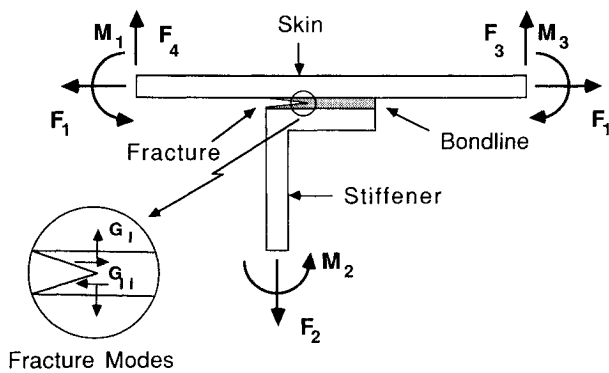


Fig. 2 Fracture of skin-stiffener joint.

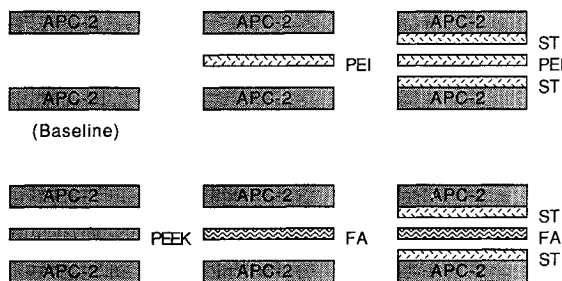


Fig. 3 Thermoplastic bonding concepts.

A great deal of work has been conducted on characterizing the fracture characteristics of APC-2 and adhesives. However, little data (mode I only) exist on the fracture characteristics of integrated thermoplastic-adhesive systems.<sup>1</sup> This study evaluates the fracture characteristics of candidate thermoplastic bonding concepts in terms of both mode I and mode II strain energy release rates. In addition, the reliability (scatter) associated with the fracture modes for each concept is addressed.

### Bonding Concepts

Five different bonding concepts were evaluated for joining unidirectional graphite thermoplastic laminates. The unidirectional material was APC-2, a poly-ether-ether-ketone (PEEK) thermoplastic reinforced with AS4 fibers. Two thermoplastic film materials, PEEK and poly-ether-imide (PEI), and an epoxy film adhesive (FA), FM-300, were used for bonding. In addition, surface treatment (ST) of the APC-2 laminates (co-consolidation with PEI film) was also considered prior to bonding with the PEI film or film adhesive materials. The five concepts along with the baseline APC-2 laminate are shown in Fig. 3.

The baseline panels were manufactured from two preconsolidated unidirectional APC-2 laminates, each of which was 16 plies thick. The two laminates were cured at 700°F and 10 psi for 30 min. For the PEEK film bonded panels, a layer of PEEK (0.010 in. thick) was added between the 16-ply APC-2 laminates prior to consolidation. The PEI film (0.005 in. thick) and film adhesive (0.010 in. thick) bonded panels were cured under vacuum with the APC-2 laminates at 550°F for 30 min and at 350°F for 60 min, respectively. The surface treated concepts were fabricated by consolidating PEI film along with the 16-ply APC-2 laminates and then bonding with the PEI film or film adhesive as previously described.

The nominal bondline thicknesses for the PEEK, PEI, and film adhesive specimens were 0.006, 0.003, and 0.009 in., respectively. The PEI and film adhesive surface treatment concepts resulted in bondline thicknesses of 0.003 and 0.011 in., respectively. These bondline thicknesses were a result of employing the previously mentioned fabrication procedures with readily available film thicknesses. No attempt was made

to establish optimum bondline thicknesses for the different concepts and fracture modes, although this parameter has been shown to play a role in the performance of adhesive systems.<sup>2,3</sup>

## Experiments

### Specimens

Double cantilever beam (DCB) and end notched flexure (ENF) specimens were fabricated from the composite panels described in the preceding section. The DCB and ENF specimen configurations with nominal dimensions are shown in Figs. 4 and 5, respectively. The DCB and ENF tests were used to quantify the mode I and mode II fracture characteristics, respectively, of the bonding concepts. Kapton inserts were used in the manufacture of the specimens to act as starter defects for the fracture tests. The inserts were 0.003 in. thick. Piano hinges were bonded to one end of the DCB specimens for load introduction, as shown in Fig. 4.

### Double Cantilever Procedure

The DCB testing was conducted quasistatically at a cross-head rate of 0.05 in./min. Load vs displacement was recorded continuously during the test until fracture initiation was visually observed. The specimen was then unloaded and the process repeated for subsequent tests at larger crack lengths (propagation data).

### End Notched Flexure Procedure

A compliance calibration was conducted for each ENF specimen prior to fracture testing. This was accomplished by placing the ENF specimens in the three-point bend fixture at  $a/L$  ratios from 0.3 to 0.8 in increments of 0.1, and measuring compliance for each crack length. Only enough load was

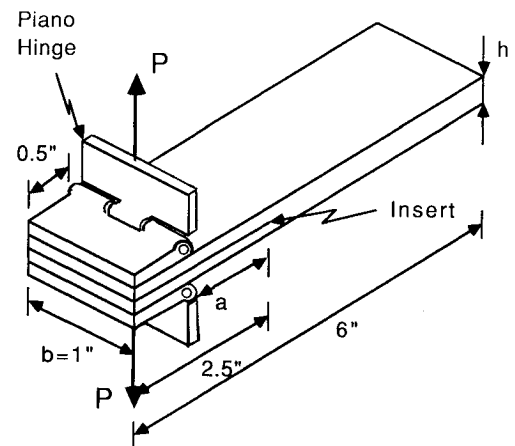


Fig. 4 Double cantilever beam specimen.

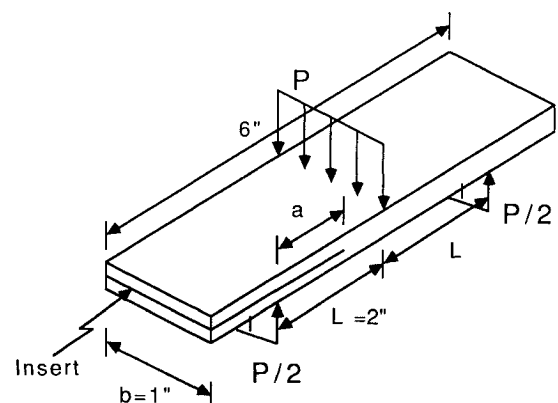


Fig. 5 End notched flexure specimen.

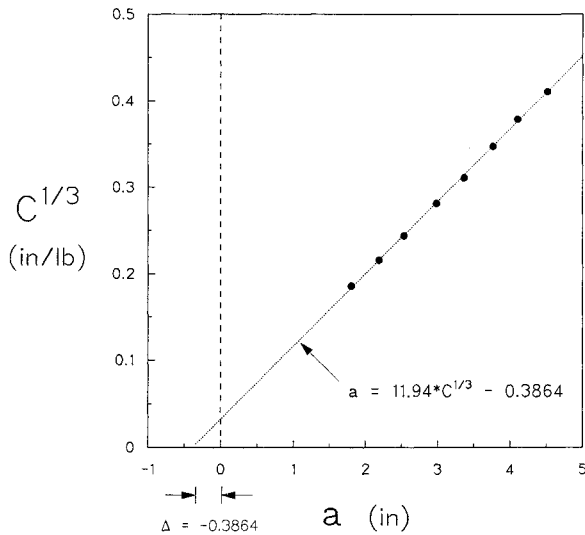


Fig. 6 Modified beam theory data.

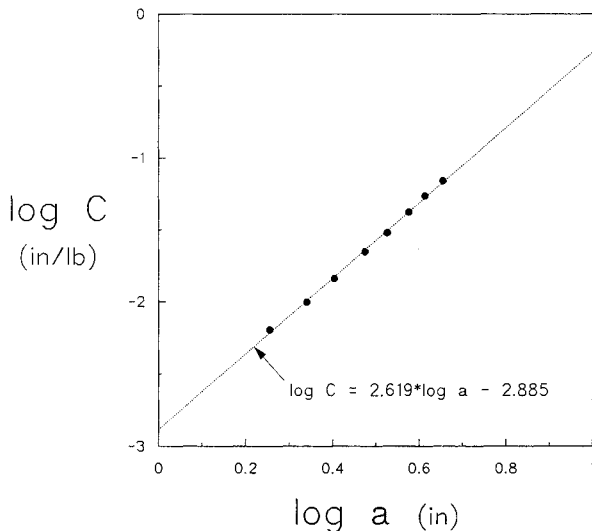


Fig. 7 Compliance calibration data.

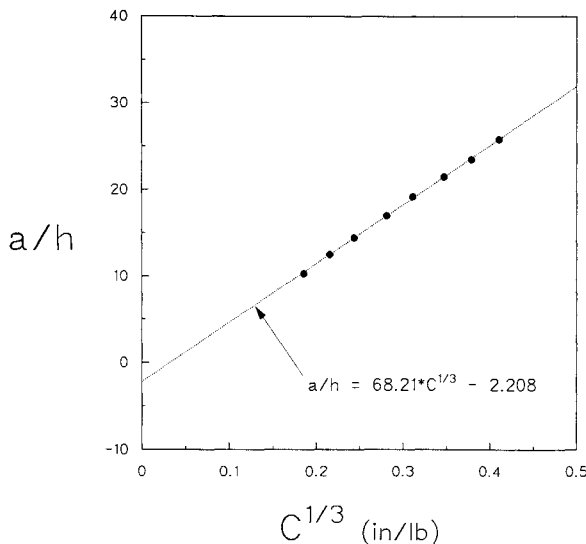


Fig. 8 Modified compliance calibration data.

applied to produce a linear load-deflection plot. Crack growth did not occur during the compliance calibration.

For fracture testing, the ENF specimens were placed in the three-point bend fixture with  $a/L = 0.8$  to limit the amount of crack growth. The specimens were then loaded at a cross-head rate of 0.1 in./min until crack growth was visually observed. As before, load vs displacement was recorded continuously during the test.

### Data Analysis

#### Double Cantilever Beam Tests

Four methods were considered for analyzing the DCB test data. They were 1) simple beam theory (BT), 2) modified beam theory (MBT), 3) a compliance calibration (CC) method, and 4) a modified compliance calibration (MCC) method. The simple beam theory expression for the strain energy release rate of a DCB specimen is

$$G_{Ic} = \frac{3P\delta}{2ba} \quad (1)$$

Typically, the simple beam theory expression overestimates the strain energy release rate. One way of correcting for this is to consider the beam as containing a crack of length  $a + |\Delta|$ , where  $\Delta$  is determined experimentally by evaluating the cube root of compliance as a function of crack length. An example of this procedure is shown in Fig. 6, where  $\Delta$  is given by the crack length axis intercept. This can be found either graphically or by performing a curve fit on the data. The fracture toughness for this modified beam theory<sup>4</sup> is then calculated using

$$G_{Ic} = \frac{3P\delta}{2b(a + |\Delta|)} \quad (2)$$

A compliance calibration method has also been used to calculate the fracture toughness of DCB specimens.<sup>5</sup> A least squares curve fit is performed on compliance vs crack length data in log-log form. The curve fit establishes the slope of the line  $m_1$ , as shown in Fig. 7. The strain energy release rate can then be determined by

$$G_{Ic} = \frac{m_1 P\delta}{2ba} \quad (3)$$

A modified compliance calibration method can also be applied to the test data.<sup>6</sup> In this procedure, the crack length is normalized by the specimen thickness  $h$  and evaluated as a function

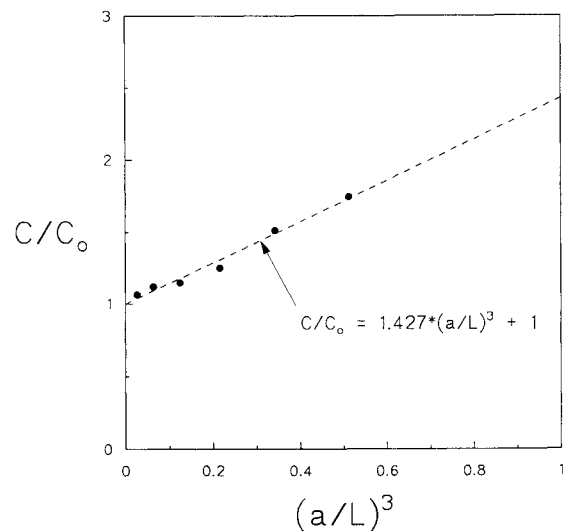


Fig. 9 ENF compliance calibration data.

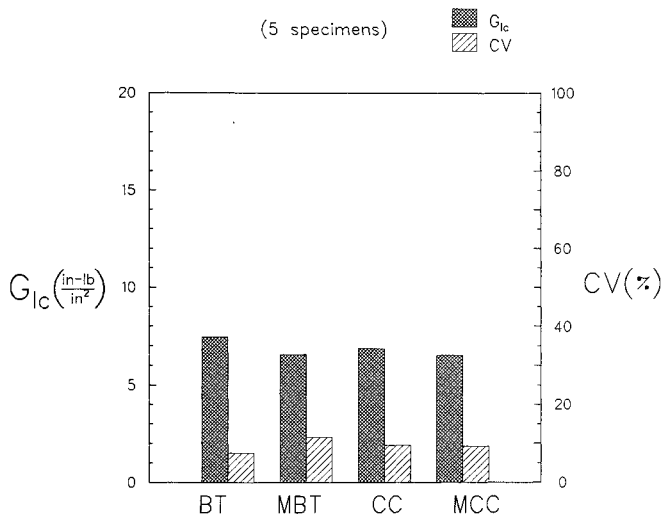
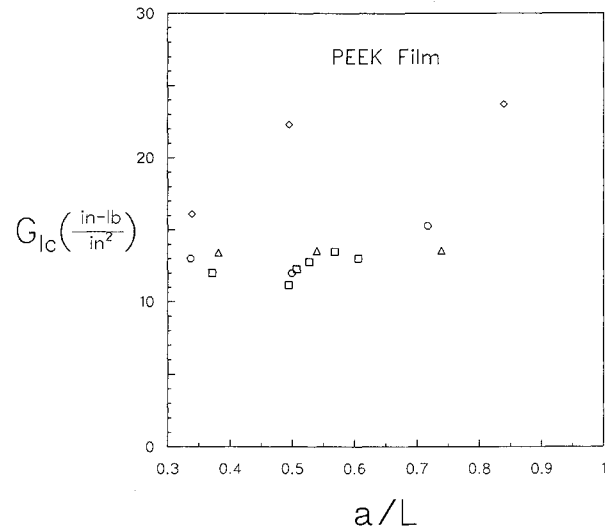
Fig. 10 APC-2  $G_{Ic}$  initiation data.

Fig. 13 PEEK film bond propagation data.

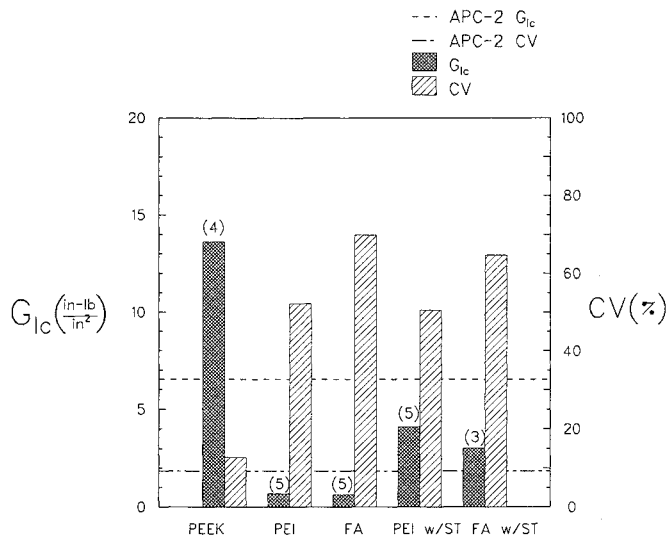
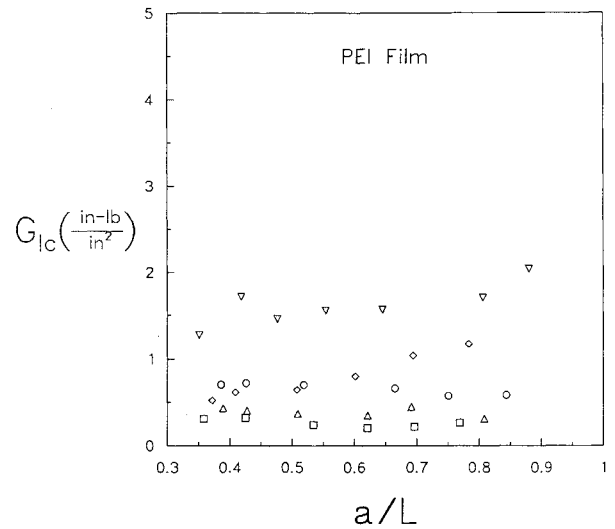
Fig. 11  $G_{Ic}$  initiation data for concepts.

Fig. 14 PEI film bond propagation data.

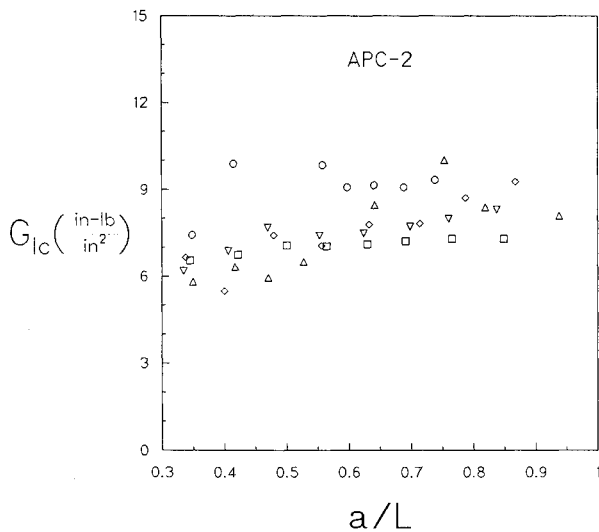


Fig. 12 APC-2 propagation data.

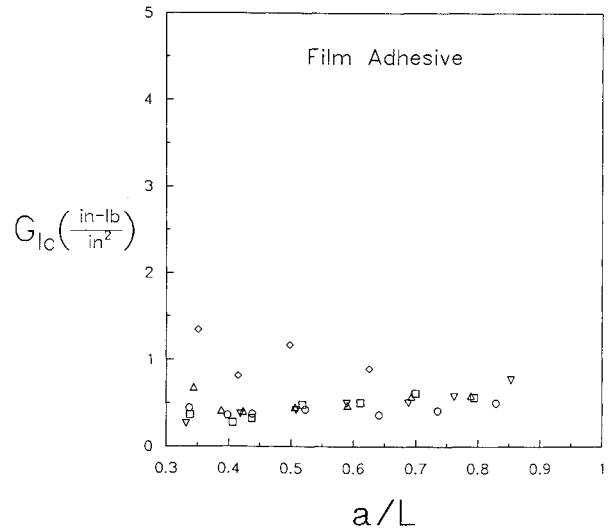


Fig. 15 Film adhesive bond propagation data.

of the cube root of compliance. As before, the data is curve fitted and the slope of the line is calculated as in Fig. 8. The fracture toughness can then be calculated by

$$G_{Ic} = \frac{3P^2C^{2/3}}{2m_2bh} \quad (4)$$

#### End Notch Flexure

Two methods were considered for calculating strain energy release rates for mode II fracture. They were 1) simple beam theory, and 2) a compliance calibration method. The beam theory expression for the ENF specimens is

$$G_{IIc} = \frac{9a^2P\delta}{2b(2L^3 + 3a^3)} \quad (5)$$

where  $L$  is the distance from the outer loading points to the center loading point.

The compliance calibration method<sup>7</sup> employs a least squares regression analysis on the compliance vs crack length data to fit an equation of the form

$$C = C_0 + m_3a^3 \quad (6)$$

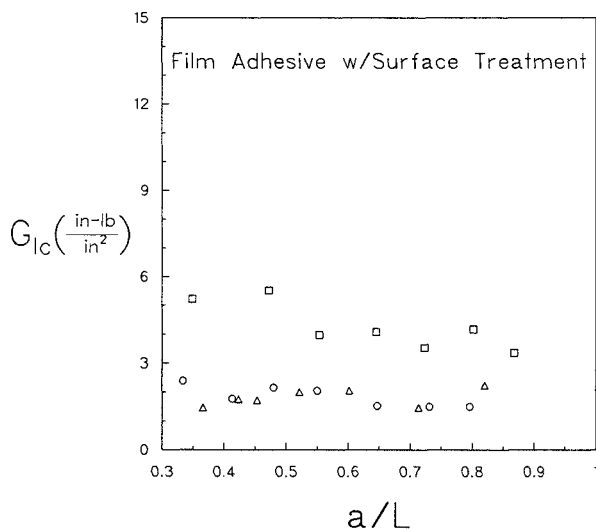


Fig. 16 Film adhesive with surface treatment propagation data.

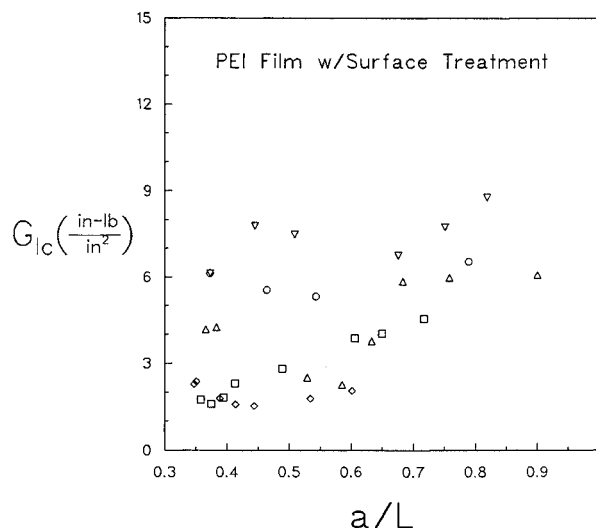


Fig. 17 PEI film with surface treatment bond propagation data.

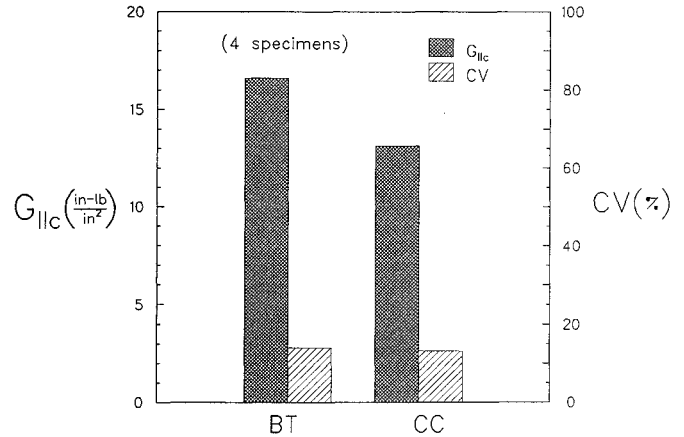


Fig. 18 APC-2  $G_{IIc}$  data.

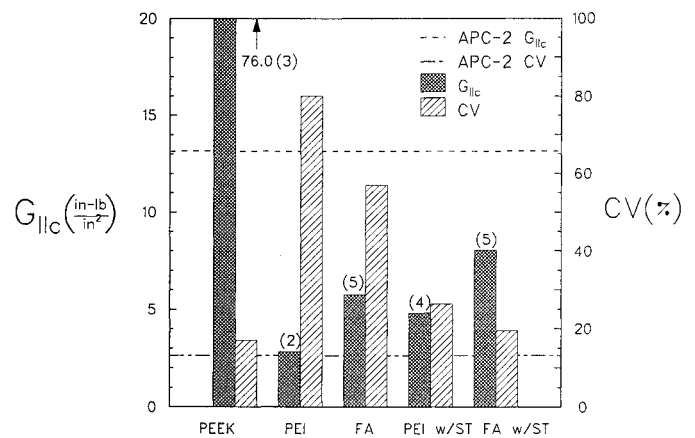


Fig. 19  $G_{IIc}$  data for concepts.

The fracture toughness is then found by using

$$G_{IIc} = \frac{3m_3P^2a^2}{2b} \quad (7)$$

Typical ENF calibration data in normalized form are shown in Fig. 9.

## Results

### Mode I Fracture

The four data analysis methods for the DCB tests were evaluated using the baseline APC-2 specimens. Initiation values for  $G_{Ic}$  were calculated for each specimen using each of the methods. The mean  $G_{Ic}$  values and coefficient of variation (CV) for each method are plotted in Fig. 10. These data compare well with other published results on APC-2, which report values of 7.6–8.3 in.-lb/in.<sup>2</sup>.<sup>8,9</sup> The modified beam theory approach and the modified compliance calibration method are shown to give the most conservative  $G_{Ic}$  values (the MCC method was 1% lower at 6.5 in.-lb/in.<sup>2</sup>). However, the scatter (CV) using the MCC method was 20% less than that of the MBT method. For these reasons, the MCC method was selected for use in comparing the bonding concepts.

The mean  $G_{Ic}$  initiation values and the data scatter for the bonding concepts are given in Fig. 11. The number of specimens tested is shown in parentheses above each  $G_{Ic}$  bar. The APC-2 data using the MCC method are also shown in the figure as broken lines.

The addition of a layer of PEEK film more than doubles the mode I fracture toughness (13.6 in.-lb/in.<sup>2</sup>) from the baseline

value, with a slight increase in scatter (see Fig. 11). However, the marked increase in  $G_{Ic}$  may be of little consequence since it merely means that the critical region shifts away from the bond to the composite material (APC-2) itself. Nevertheless, the potential payoff of adding PEEK film in highly loaded areas that can be coconsolidated with the composite material (e.g., curved sections that are prone to delamination) is apparent. The  $G_{Ic}$  value for this concept compares well with other published data on PEEK film bonds<sup>1</sup> ( $G_{Ic} = 12.8$  in.-lb/in.<sup>2</sup>).

Bonding with PEI film and film adhesive significantly decreases the mode I fracture toughness and greatly increases data scatter when compared with the baseline material, as shown in Fig. 11. Mean  $G_{Ic}$  values for the PEI and film adhesive bonds are reduced by over 90% to 0.68 and 0.62 in.-lb/in.<sup>2</sup>, respectively. The opening mode performance of the film adhesive bond is slightly greater than other available data on one-part epoxies<sup>1</sup> ( $G_{Ic} = 0.1$ – $0.2$  in.-lb/in.<sup>2</sup>).

The incorporation of PEI surface treatment prior to bonding with PEI film or film adhesive significantly improves the fracture toughness compared to using the PEI film or film adhesive alone (see Fig. 11). The mean  $G_{Ic}$  values for the PEI and film adhesive surface treatment concepts are 4.1 and 3.0 in.-lb/in.<sup>2</sup>, respectively. In addition, the scatter is reduced when surface treatment is employed. However, the scatter remains high relative to the composite material.

Propagation  $G_{Ic}$  values for the APC-2 and bonding concept specimens are shown in the form of delamination resistance plots in Figs. 12–17. Different symbols are used for each specimen, and strain energy release rates corresponding to various  $a/L$  ratios are plotted.

The delamination resistance data for the APC-2 specimens (Fig. 12) show a trend toward higher  $G_{Ic}$  values and reach a plateau at an  $a/L$  of about 0.6. This apparent toughening is caused by fiber bridging, i.e., the pulling of fibers from one side of the delamination plane to the other. Although this can be viewed as representative of fracture in the actual structure, the higher toughness values may be nonconservative if bridging fails to occur.<sup>10</sup> The propagation data compare well with other published results.<sup>8,9,11,12</sup>

Except for one specimen, the PEEK film bond does not appear to show any signs of toughening with increasing crack length (Fig. 13). This is not conclusive since few tests were conducted at the larger crack lengths ( $a/L > 0.7$ ). However, the  $G_{Ic}$  values are significantly higher than the APC-2 laminates, due in part to the cohesive failure of the tough PEEK bond.

The PEI film, film adhesive, and film adhesive with surface treatment results in Figs. 14, 15, and 16, respectively, also indicate nearly constant  $G_{Ic}$  values for all crack lengths. All of these bonding concepts failed adhesively (at the interface between the bonding and composite materials).

The PEI film with surface treatment appears to show an increase in fracture toughness as  $a/L$  increases beyond 0.6 (Fig. 17). In fact, the  $G_{Ic}$  values for  $a/L > 0.65$  approach or exceed the  $G_{Ic}$  onset value of the APC-2 system. This may be due to plastic deformation of the amorphous PEI material in the crack-tip region. Furthermore, the scatter in the calculations appears to decrease somewhat at the larger crack lengths. The high  $G_{Ic}$  values for this bonding concept relative to the other non-PEEK concepts may be due to the cohesive nature of the fracture process.

#### Mode II Fracture

The two ENF data analysis methods were evaluated on the APC-2 specimens. The average mode II strain energy release rates using the beam theory and compliance calibration analysis methods are shown in Fig. 18. The compliance calibration method produces a more conservative  $G_{IIc}$  value (13.1 in.-lb/in.<sup>2</sup>), which is 21% less than the beam theory value (16.6 in.-lb/in.<sup>2</sup>). In addition, the scatter of the  $G_{IIc}$  calculations is slightly less using the compliance calibration method (CV of

13% vs 14%). Therefore, the compliance calibration method was selected for use in comparing the strain energy release rates of the bonding concepts. Other published results for mode II fracture of APC-2 report values of 8.6–14.2 in.-lb/in.<sup>2, 8,9,11,12</sup>

Mean values for the mode II strain energy release rates of the bonding concepts are shown in Fig. 19. The scatter in the calculations and the APC-2 data are also given in the figure. The number of specimens tested for each concept is shown in parentheses above the mean value.

Bonding with PEEK film increases the mode II strain energy release rate by nearly six times compared to the APC-2 laminates. Furthermore, the relative increase in data scatter is minimal. For mode II loaded structures, reinforcing critical areas with PEEK film may be desirable if the structural design allows for consolidation with the composite material.

The PEI film and film adhesive concepts produced mean strain energy release rates of 2.8 and 5.7 in.-lb/in.<sup>2</sup>, respectively. The results for these concepts also show large scatter (CV > 50%) in the  $G_{IIc}$  calculations relative to the APC-2 laminates.

The incorporation of PEI surface treatment prior to bonding with the PEI film and the film adhesive significantly improves the bonding performance. The  $G_{IIc}$  values for the PEI film and film adhesive concepts with surface treatment increase to 4.8 and 8.0 in.-lb/in.<sup>2</sup>, respectively. This amounts to increases in  $G_{IIc}$  of 71 and 40%, respectively, over the concepts without surface treatment. The decrease in scatter with the use of surface treatment is also quite significant. The PEI film and film adhesive concepts with surface treatment produce coefficients of variation of 26 and 19%, respectively. This represents a reduction in scatter to one-third that of the concepts without surface treatment.

#### Conclusions

The conclusions from this experimental study may be summarized as follows.

- 1) Adding PEEK film in highly loaded areas that can be consolidated with the APC-2 can significantly increase both the mode I and mode II fracture toughness (+110 and +480%, respectively) relative to the baseline material.
- 2) Coconsolidating PEI with APC-2 prior to bonding with film adhesive or PEI film improves the mode I performance (+380 and +500%, respectively) and the mode II performance (+40 and +71%, respectively) and reduces data scatter compared to bonding with the films alone.
- 3) With the exception of the PEEK film bond, high data scatter (coefficient of variations > 50%) is inherent in the mode I fracture of the bonding concepts.

#### References

- <sup>1</sup>Kodokian, G. K. A., and Kinloch, A. J., "The Adhesive Fracture Energy of Bonded Thermoplastic Fibre-Composites," edited by L. H. Sharpe and S. E. Wentworth, *The Science and Technology of Bonding, Proceedings of the 35th Sagamore Army Materials Research Conference*, Gordon & Breach, New York, 1990, pp. 193–218.
- <sup>2</sup>Chai, H., "Bond Thickness Effect in Adhesive Joints and Its Significance for Mode I Interlaminar Fracture of Composites," *Composite Materials: Testing and Design (Seventh Conference)*, edited by J. M. Whitney, American Society for Testing and Materials, ASTM STP 893, Philadelphia, PA, 1986, pp. 209–231.
- <sup>3</sup>Chai, H., "Shear Fracture," *International Journal of Fracture*, Vol. 37, 1988, pp. 137–159.
- <sup>4</sup>Hashemi, S., Kinloch, A. J., and Williams, J. G., "Corrections Needed in Double Cantilever Beam Tests for Assessing the Interlaminar Failure of Fibre-Composites," *Journal of Materials Science Letters*, Vol. 8, 1989, pp. 125–129.
- <sup>5</sup>Berry, J. P., "Determination of Fracture Energies by the Cleavage Technique," *Journal of Applied Physics*, Vol. 34, No. 1, 1963, pp. 62–68.
- <sup>6</sup>Kageyama, K., "Proposed Methods for Interlaminar Fracture Toughness Tests of Composite Laminates," *Proceedings of the 5th U.S./Japan Conference on Composite Materials*, Tokyo, June 1990.

<sup>7</sup>O'Brien, T. K., Murri, G. B., and Salpekar, S. A., "Interlaminar Shear Fracture Toughness and Fatigue Thresholds for Composite Materials," *Composite Materials: Fatigue and Fracture*, edited by P. A. Lagace, Vol. 2, ASTM STP 1012, American Society for Testing and Materials, Philadelphia, PA, 1989, pp. 222-250.

<sup>8</sup>Prel, Y. J., Davies, P., Benzeggagh, M. L., and deCharentenay, F. X., "Mode I and Mode II Delamination of Thermosetting and Thermoplastic Composites," *Composite Materials: Fatigue and Fracture*, edited by P. A. Lagace, Vol. 2, ASTM STP 1012, American Society for Testing and Materials, Philadelphia, PA, 1989, pp. 251-269.

<sup>9</sup>Russell, A. J., and Street, K. N., "The Effect of Matrix Toughness on Delamination: Static and Fatigue Fracture Under Mode II Shear Loading of Graphite Fiber Composites," *Toughened Composites*, edited by N. J. Johnston, STP 937, American Society for Testing and

Materials, Philadelphia, PA, 1987, pp. 275-294.

<sup>10</sup>Johnson, W. S., and Mangalgiri, P. D., "Investigation of Fiber Bridging in Double Cantilever Beam Specimens," *Journal of Composites Technology and Research*, Vol. 9, No. 1, 1987, pp. 10-13.

<sup>11</sup>Mall, S., Yun, K. T., and Kochhar, N. K., "Characterization of Matrix Toughness Effect on Cyclic Delamination Growth in Fiber Composites," *Composite Materials: Fatigue and Fracture*, edited by P. A. Lagace, Vol. 2, ASTM STP 1012, American Society for Testing and Materials, Philadelphia, PA, 1989, pp. 296-310.

<sup>12</sup>Martin, R. H., and Murri, G. B., "Characterization of Mode I and Mode II Delamination Growth and Thresholds in AS4/PEEK Composites," *Composite Materials: Testing and Design*, edited by S. P. Garbo, Vol. 9, ASTM STP 1059, American Society for Testing and Materials, 1990, p. 251-270.

## International Reference Guide to Space Launch Systems

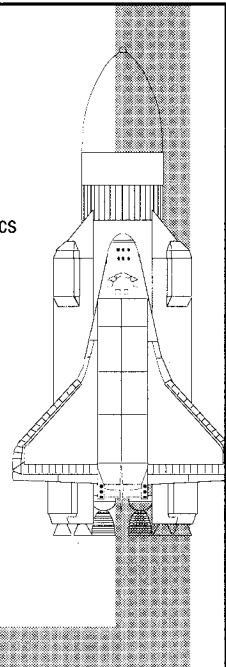
1991 Edition *Compiled by Steven J. Isakowitz*

In collaboration with the  
American Institute of Aeronautics and Astronautics  
Space Transportation Technical Committee

"Best book on the market." — Charles Gunn, Director Unmanned Launch Vehicles, NASA Headquarters

This authoritative reference guide summarizes the proliferation of the launch programs for China, Europe, India, Israel, Japan, the Soviet Union, and the United States. The guide contains a standard format for each launch system, including: historical data; launch record; price data; descriptions of the overall vehicle, stages, payload fairing, avionics, attitude control system; performance curves for a variety of orbits; illustrations of launch site, facilities, and processing; flight sequence and payload accommodations. The text is a quick and easy data retrieval source for policymakers, planners, engineers, and students.

1991, 295 pp, illus, Paperback • ISBN 1-56347-002-0  
AIAA Members \$25.00 • Nonmembers \$40.00 • Order No. 02-0 (830)ü



Place your order today! Call 1-800/682-AIAA



American Institute of Aeronautics and Astronautics  
Publications Customer Service, 9 Jay Gould Ct., P.O. Box 753, Waldorf, MD 20604  
Phone 301/645-5643, Dept. 415, FAX 301/843-0159

Sales Tax: CA residents, 8.25%; DC, 6%. For shipping and handling add \$4.75 for 1-4 books (call for rates for higher quantities). Orders under \$50.00 must be prepaid. Please allow 4 weeks for delivery. Prices are subject to change without notice. Returns will be accepted within 15 days.